Simulation Study of Toroidal Flow Generation by the ICRF Minority Heating

S. Murakami[1)], K. Itoh[2)], L.J. Zheng[3)], J.W. Van Dam[3)], A. Fukuyama[1)]

[1)] *Departiment of Nuclear Engineering, Kyoto University, Sakyo, Kyoto 606-8501, Japan*
[2)] *National Institute for Fusion Science, 322-6 Oroshi, Toki 509-5292, Japan*
[3)] *Institute for Fusion Studies, The Univ. of Texas at Austin, Austin, Texas 78712-0262, USA*

E-mail contact of main author: murakami@nucleng.kyoto-u.ac.jp

Abstract. The toroidal flow generation by the ICRF minority heating is investigated in the Alcator C-mod like plasma applying GNET code, in which the drift kinetic equation is solved in 5D phase-space. An asymmetry of distribution function in the parallel direction is found and two kinds of toroidal flow are observed. One is the sheared flow near the RF power absorption region depending on the sign of $k_{\|}$. The other is the toroidal flow, which is larger than the previous one, independent of the sign of $k_{\|}$. Additionally the toroidal flow reversal from co to counter direction is obtained when we change the toroidal current to the opposite direction. These facts indicate that there exists two kinds of the driving mechanism of toroidal flow. Two models to explain the obtained toroidal flow are studied. We find that the toroidal motions of energetic tail ions caused by the finite banana effect in the finite magnetic shear and, also, by the poloidal magnetic drift plays important role in the generation of the toroidal flow.

1. Introduction

Important role of the plasma flow and its shear in the transport improvement is suggested by many experimental observations, e.g. H-mode transition, ITB formation, RWM suppression. In a future reactor the driving of the plasma flow by NBI heating is not efficient and other driving method is required. The spontaneous toroidal flow has been observed during ICRF heating with no direct momentum input in JET[1], Alcator C-mod[2] and etc. Many theoretical studies have been done. However, further study is necessary to make clear the generating mechanism of spontaneous toroidal flow during ICRF heating.

Recently toroidal sheared flow generation model by a local ICRF heating is proposed by Ohkawa and Miller[3]. Assuming the ICRF waves with an asymmetric wave number, resonant ions lose their toroidal momentum due to the transition from the passing to the trapped particle and, then, the opposite direction toroidal flow would be generated. Similar mechanism has been proposed in ECH and has been confirmed experimentally known as "Ohkawa" current. But, in the ICRF heating, there are differences from ECH mechanism such as multiple interaction with RF waves and small pitch angle scattering effect. Also this model is based on the simplified theory. Thus the investigation of this model by a realistic simulation is required.

In this paper we study the toroidal flow generation by the ICRF heating using GNET code[4, 5], which can solve a linearized drift kinetic equation for energetic ions including complicated behavior of trapped particles in 5-D phase space. The obtained steady state distribution of energetic minority ions is analyzed and the radial profile of the toroidal flow is evaluated. In the simulation we assume a tokamak plasma similar to the Alcator C-mod plasma ($R = 0.67$m, $r \sim 0.21$m, $B_t \sim 5.5$T) as a first step.

2. Simulation Model

In order to study the ICRF minority heating including finite orbit effect we have developed a global simulation code, GNET[4, 5], which can solve a linearized drift kinetic equation for energetic minority ions, $f_{\rm min}$, including complicated behavior of trapped particles in 5-D phase space

$$\frac{\partial f_{\rm min}}{\partial t} + (v_\parallel + v_D)\cdot\nabla f_{\rm min} + \boldsymbol{a}\cdot\nabla\boldsymbol{v} f_{\rm min} - C(f_{\rm min}) - Q_{\rm ICRF}(f_{\rm min}) - L_{\rm particle} = S_{\rm particle} \quad (1)$$

where $C(f_{\rm min})$ and $Q_{\rm ICRF}(f_{\rm min})$ are the linear Coulomb Collision operator and the ICRF heating term. $S_{\rm particle}$ is the particle source term by ionization of neutral particle and the radial profile of the source is evaluated using AURORA code. The particle sink (loss) term, $L_{\rm particle}$, consists of two parts; one is the loss by the charge exchange loss assuming the same neutral particle profile as the source term calculation and the other is the loss by the orbit loss escaping outside of outermost flux surface.

The $Q_{\rm ICRF}$ term is modeled by the Monte Carlo method. When the test particle pass through the resonance layer, $\Omega_c = \omega_R F - k_\parallel v_\parallel$, the perpendicular velocity of this particle is changed. The code can include the multi waves that have different wave numbers.

Using GNET code we study the toroidal shear flow generation by ICRF minority heating in the Alcator C-mod Plasma. The RF electric field amplitude is assumed to be $|E^+| = E_0^+ \tanh\{C_r(1 - r/a)\}\exp\{-(\sin\theta/C_\theta)^2\}$, where θ is the poloidal angle and we set $C_r = 0.3$ and$C_\theta = 0.3$. This RF electric field model generates the local ICRF heating region near the equatorial plane as assumed in the Ohkawa model. Also the resonant magnetic field strength B_{res} is set to be 5.1T and the location of the resonance in the minor radius, r, is about $r/a = 0.3$.

3. Simulation results

We perform the simulation using GNET code until we obtain a steady state distribution of energetic minority ions solving Eq. (1). We assume the following plasma parameters; $n_{e0} \sim 8\times10^{19}$m^{-3}, $T_0 \sim 3.2$keV and B_0=5.4T. The amplitude of RF electric field, E_0^+, is set to 3.0kV/m, which corresponds to the heating power of 0.35MW. The parallel wave number, $k_\parallel$, is assumed to be $\left|k_\parallel\right| = 5$m^{-1} and the perpendicular wave number is $k_\perp$ =50m^{-1}.

Figure 1 shows the radial profile of the RF power absorption (a), heat power deposition (b), and energetic ion pressure (c). We can see a peaked absorption profile of RF wave power near $r/a \sim 0.3$ while a broader heat deposition profile for electron an ions. This indicates the existence of the radial diffusion of energetic ions due to the finite orbit effect. The minority density profile is a flat profile but energetic ion pressure profile shows a peak similar to the electron heat deposition one.

Next we evaluate the velocity distribution function of the minority ions during the ICRF heating. Figure 2 shows the flux averaged velocity space distribution of the minority ion in the different minor radius region; (a) $r/a = 0.4$ to 0.5 and (b) $r/a = 0.6$ to 0.7. The minority ions are accelerated perpendicular direction by the RF wave interaction and we can see a tail ion formation due to the ICRF heating. Interestingly we can see strong asymmetry in the parallel velocity direction. This asymmetry enlarges in the radial region $r/a \sim 0.7$ and the total distribution also shows an asymmetry. These indicate the existence of a net toroidal flow driven by the ICRF heating.

The toroidal flow is evaluated integrating the distribution function with the weight of the local toroidal velocity. Figure 3-(a) (blue solid line) shows the radial profile of the toroidal flow driven by the ICRF heating. We can see a toroidal flow which has a peak near $r/a \sim 0.4$. The direction of the toroidal flow is the co-direction, which is consistent with the experimental observation in the Alcator C-mod plasma.

We next study the $k_\parallel$ sign dependency of the toroidal flow velocity because the flow by Ohkawa model depends on the sign of $k_\parallel$. Figure 3-(a) (red dashed line) shows the toroidal flow with the negative $k_\parallel$ cases, $k_\parallel = -5\text{m}^{-1}$. A difference in the toroidal flow near $r/a \sim 0.3$ (P_{abs} peak position) is observed but no clear difference can be seen in the P_{abs} and P_{dep}. In order to make clear the $k_\parallel$ sign dependence in the flow we evaluate a difference between two cases in the Fig. 3-(b). We can see a clear difference near $r/a \sim 0.3$, RF wave absorption region, and the flow direction changes from negative to positive at this point. This would be related to the Ohkawa model. The results still contain relatively large noise so we will do more precise simulation to make clear this point. On the other hand we found that dominant part of the flow dose not depend on the $k_\parallel$ sign. If we use the symmetric $k_\parallel$ waves, in this case Ohkawa drive disappear, but we can see a flow similar to the one in the asymmetric wave number case.

We, next, investigate the direction change of the toroidal flow reversing the toroidal current. The toroidal flow reversal has been observed in Alcator C-mod experiments when the toroidal current changes the direction. We perform the simulation with the opposite direction toroidal current. When we change the direction of the toroidal current, the flux averaged distributions function shows an opposite asymmetric distribution from that of the previous case. Then, the toroidal flow reversal has been also observed in Fig. 3-(c). This flow direction change is consistent with the experimental observation in the Alcator C-mod.

4. Theoretical Analysis

To consider the mechanism to generate obtained toroidal flow by ICRF heating we start from the guiding center motion of energetic minority ions. When we plot the toroidal position as a function of time we can see net toroidal motions which strongly depend on the energy. We think that this toroidal motion would play an important role in the observed toroidal flow.

The average toroidal motion of energetic ion is given by

$$\bar{\dot{\zeta}} = \frac{1}{T}\oint dt\dot{\zeta} = \frac{1}{T}\oint d\theta\frac{\dot{\zeta}}{\dot{\theta}}. \tag{2}$$

Substituting the equations for the poloidal and toroidal motions in the Boozer coordinates to Eq. (2) we obtain[6]

$$\bar{\dot{\zeta}} \simeq \frac{1}{T}\oint q d\theta - \frac{1}{T}\oint d\theta\Delta q(gq+I) + \frac{1}{T}\oint d\theta\rho_c q(g'q+I'). \tag{3}$$

where $\Delta = m\delta B'/e^2B^2\rho_c$ and $\delta = e^2\rho_c^2 B/m + \mu$. We ignore the higher oder terms $O\ (r/R)^2$.

There are three important components in the Eq. (5). First term is the net toroidal motion due to the finite banana width in the finite magnetic shear. When there is a magnetic shear the particle run on the different safety factor magnetic field in one bounce of banana motion. Second term is due to the poloidal and toroidal drift. Actually poloidal drift generate the imbalance of time between going and back motions of banana bounce motion. The same direction motion with the poloidal drift takes shorter time than that of opposite direction one and this means that the net toroidal motion occurs due to the time difference between them. The third time is normally small term and we will ignore here. We evaluate the toroidal motion changing the these effects in Fig. 5. We plot the cases without magnetic shear, without poloidal drift, and no shear and no poloidal drift cases. We can see the poloidal drift effect is larger than the others.

We now assume a simple tokamak configuration as $B(r, \theta) = B_0\{1 - (r/R)\cos\theta\}$. We obtain

$$\begin{aligned} \bar{\dot{\zeta}} &\simeq \frac{4qsmv^2}{rReB_0}\frac{gq}{gq-I}\frac{E(\kappa)+(\kappa^2-1)K(\kappa)}{K(\kappa)} \\ &\quad + \frac{qmv^2}{2rReB_0}\frac{gq+I}{gq-I}\frac{2E(\kappa)-K(\kappa)}{K(\kappa)}, \end{aligned} \tag{4}$$

where $\kappa = \sin(\theta_b/2)$, and $K(\kappa)$ and $E(\kappa)$ are the first and second kind of elliptic integrals. And $q' = (dq/d\psi) = qs/r^2B_0$ and $s = r(dq/dr)/q$. If we consider a limit $\kappa << 1$ the toroidal precession is approximately given by

$$\bar{\dot{\zeta}} \simeq \frac{4qsE\kappa^2}{rReB_0} + \frac{qE(1-\kappa^2)}{rReB_0} \tag{5}$$

The obtained net toroidal motion dose not depend on the wave number of RF waves and the direction is reversed when the toroidal current direction is changed. This would be a mechanism to drive the obtained toroidal flow independent of $k_\parallel$. Using Eq. (7) we estimate the toroidal flow in the simulated case. The net toroidal flow is calculated as

$$< \bar{\dot{\zeta}} > = \frac{\int \bar{\dot{\zeta}}(E) f_{\min}(E) dE}{\int f_{\min}(E) dE}, \tag{6}$$

where $f_{\min}$ is the energy distribution obtained by GNET simulation. Figure 6 shows the estimated toroidal flow applying Eq. (8). We obtain relatively good agreement between the GNET result and the estimated one. This indicates that the obtained $k_\parallel$ independent toroidal flow is driven by the net toroidal motion of energetic tail ions.

5. Conclusions

We have studied the toroidal sheared flow generation by the ICRF minority heating applying GNET code, in which the drift kinetic equation is solved in 5D phase-space, to the Alcator C-mod like plasma. We have found an asymmetry of velocity distribution function in the parallel direction and obtained two kinds of toroidal flows. One is the sheared flow near the RF power absorption region ($r/a \sim 0.3$) depending on the sign of $k_\parallel$. The other is the toroidal flow, which is larger than the previous one, independent of the sign of $k_\parallel$. The simulation result with the symmetric $k_\parallel$ heating also shows a toroidal flow similar to that in the asymmetric $k_\parallel$ case. Additionally the toroidal flow reversal from co to counter direction has been observed when we change the toroidal current to the opposite direction. These facts indicate that there exists two kinds of the driving mechanism of toroidal flow.

The one which has a $k_{\parallel}$ dependence would be related to the mechanism proposed by Ohkawa et al.[3]. The quantitative comparisons with Ohakawa model wold be done in future. In order to make clear the other toroidal flow mechanism which is dominant in the simulation results we have studied the net toroidal motion of trapped tail ions. Using obtained form of the net toroidal motion of trapped tail ions we have estimated the averaged velocity of minority ions. We have obtained relatively good agreement between the GNET result and the estimated one. This indicates that the obtained $k_{\parallel}$ independent toroidal flow is driven by the net toroidal motion of energetic tail ions.

References

[1] L-G. Eriksson, Plasma Phys. Control. Fusion 39 (1997) 27.

[2] J.E. Rice et al., Nucl. Fusion 45 (2005) 251.

[3] T. Ohkawa, Phys. Plasmas 12 (2005) 094506.

[4] S. Murakami, et al., Nucl. Fusion 40 (2000) 693.

[5] S. Murakami, et al., Nucl. Fusion 46 (2006) S425.

[6] R.B. White, "The Theory of Toroidally Confined Plasmas", Imperial College Press (2001), p84.

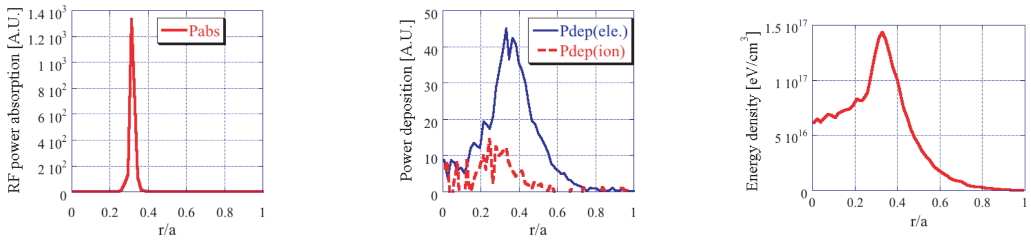

Figure 1: Radial profile of (a) the RF wave power absorption, (b) the power depositions for electron and ion, and (c) the minority ion pressure.

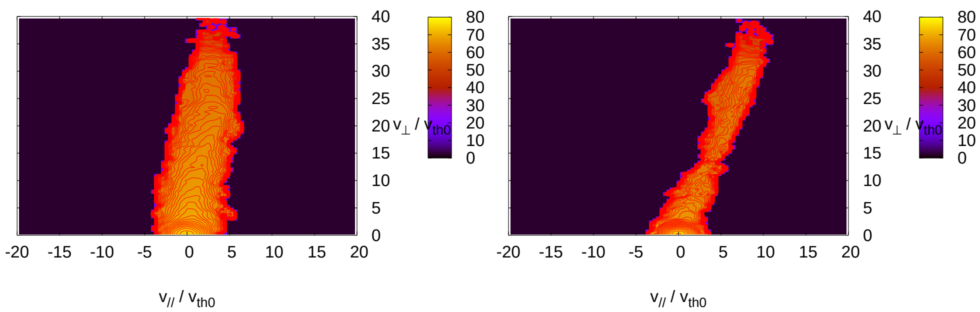

Figure 2: Contour of the flux surface averaged velocity space distribution, $\ln f_{min}$, of the minority ion at the different radial regions; $r/a = 0.4 \sim 0.5$ (left) and $0.6 \sim 0.7$ (right).

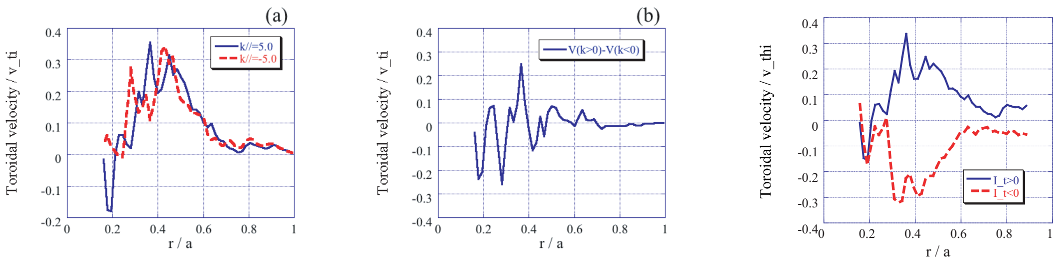

Figure 3: Radial profile of averaged toroidal velocities of minority ions; (a) the $k_{\parallel}$ =5 and -5 m^{-1} case, (b) the difference $V(k_{\parallel} = 5) - V(k_{\parallel} = -5)$ and (c) the toroidal current reversal

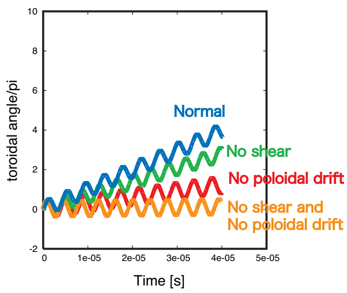

Figure 4: Toroidal angle position of typical energetic trapped ions as a function of time with different conditions; normal, no magnetic shear, no poloidal drift, and no magnetic shear+no poloidal drift.

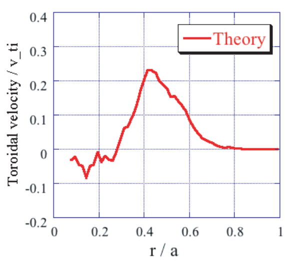

Figure 5: Radail profile of the estimated toroidal flow by the net toroidal drift motion.